

Damping of the soft *E*-symmetry phonon in lead titanate

D. Heiman* and S. Ushioda

Department of Physics, University of California, Irvine, California 92717

(Received 24 November 1975; revised manuscript received 14 April 1977)

The frequency and temperature dependence of the phonon damping function $\gamma(\omega, T)$ of the soft *E*-symmetry phonon in PbTiO_3 has been determined using Raman scattering. From 40°K to room temperature the frequency of the lowest *E* mode, $\omega_0(T)$, is nearly constant and permits the temperature dependence of γ to be measured at constant frequency. Below room temperature, $\gamma(\omega_0, T)$ is proportional to the absolute temperature T and extrapolates to zero damping at $T = 0$. The frequency dependence of $\gamma(\omega, T_{\text{rm}})$ was determined at room temperature using near-forward Raman scattering from polaritons. New results are obtained by reanalyzing previously reported data. The damping is found to increase for decreasing polariton frequencies down to about 53 cm^{-1} . Below the ferroelectric phase transition at 766°K, it is shown that the apparent divergence of $\gamma(\omega_0(T))$ as $T \rightarrow T_c^-$ results mainly from this frequency dependence and a nearly linear dependence on temperature. At fixed frequency, $\gamma(\omega, T)$ is proportional to the absolute temperature although smaller nonlinear contributions cannot be ruled out. This linear temperature dependence indicates that the dominant damping mechanism for the soft *E* mode is due to cubic anharmonicity in the lattice potential. These results are interpreted in terms of the model described by Cowley for phase transitions arising from anharmonic decay. A review of experimental results concerning the temperature dependence of the damping of soft modes in related materials is included.

INTRODUCTION

There is considerable interest in the anharmonic processes involved in the decay or scattering of soft modes in displacive phase transitions. The anharmonicity in the crystal potential energy not only accounts for the finite lifetime of the vibrational modes but is also believed to be the cause of the softening of the mode, bringing about a transition to a new phase.¹⁻³

The anharmonicity causes a complex shift in the harmonic vibrational frequency Ω_0 and is conveniently described by the phonon self-energy $\Sigma(\vec{q}, \omega, T) = \Delta - i\Gamma$.⁴ The real part Δ causes the harmonic vibrational frequency to vary strongly with temperature and the imaginary part Γ determines the inverse lifetime of the phonon. The renormalized soft-mode frequency is given by $\omega_0^2 = \Omega_0^2 + 2\Omega_0\Delta$. The frequency and temperature dependence of the phonon-damping function $\gamma(\omega, T)$, which is related to the imaginary part of Σ by $\Gamma = \omega\gamma/2\Omega_0$, is important in understanding the nature of phase transitions.

Measurements of the temperature dependence of the damping or linewidth of soft modes, $\gamma(\omega_0(T))$, have been performed on SrTiO_3 and KTaO_3 ,⁵ above the transition temperature T_c , and on GeTe ,⁶ PbTiO_3 ,⁷ SrTiO_3 ,⁸ KMnF_3 ,⁹ AlAsO_4 ,¹⁰ $\text{Gd}_2(\text{MoO}_4)_3$,¹¹ and¹² BaMnF_4 below T_c . In all these materials $\gamma(\omega_0(T))$ increases with increasing T , although the analytic dependences are not clear; in some cases $\gamma(T)$ appears to have a divergent behavior as T_c is approached from below. The lowest *E* mode in PbTiO_3 is particularly useful for study; it has a

large scattering strength which increases as the transition is approached, and moderate damping, although still underdamped. Burns and Scott¹³ observed that $\gamma(\omega_0(T))$ increased in a divergent manner as $T \rightarrow T_c^-$. They related the dependence to an empirical relation similar to that found for the dielectric constant along the ferroelectric axis $\epsilon_c(0)$, which also diverges. Subsequently, Silverman¹⁴ suggested a theory to explain the anomalous divergence of $\gamma(\omega_0(T))$. In this theory damping increases as the soft-mode frequency $\omega_0(T)$ becomes closer to a resonance with an LA-TA scattering process near the zone center.

The problem in studying the temperature dependence of γ for a soft mode is that both the temperature and the frequency are changing simultaneously. One purpose of this study is to determine the nature of the anomalous behavior in $\gamma(\omega_0, T)$ by obtaining the frequency and temperature dependence separately. The frequency dependence of γ at room temperature is determined by measuring the polariton linewidths at various polariton frequencies ω_{\pm} and relating these to $\gamma(\omega_{\pm}, T_{\text{rm}})$. The pure temperature dependence, at nearly constant frequency, was obtained by measuring γ in a backscattering geometry below room temperature where $\omega_0(T)$ changes little with temperature. The temperature dependence of ω_0 was also accurately measured below room temperature. From the temperature dependence of γ the dominant damping mechanism can be inferred, while the frequency dependence helps to identify the particular decay or scattering channel involved. Also, by comparing the frequency dependence of the damping of

the lowest *E*-symmetry mode in PbTiO₃ with that of the closely related isomorph BaTiO₃, some insight is gained concerning the reason for the very large damping observed in BaTiO₃.¹⁵ An accurate value for the low-frequency dielectric constant along a direction perpendicular to the ferroelectric *c* axis, $\epsilon_a(0)$, is also extracted from the polariton peak position. This value is then compared with that derived from the Lyddane-Sachs-Teller (LST) relation. Finally, experimental results concerning temperature-dependent damping of the soft modes, associated with structural phase transitions in related materials, is reviewed. The divergent damping found in other materials is reexamined in light of the results of the present experiment.

THEORY

The Raman scattering cross section $S(q, \omega)$ for polaritons of wave vector q and frequency ω can be calculated directly from a response-function method employed by Benson and Mills,¹⁶ and Barker and Loudon.¹⁷ The total cross section for Stokes scattering is given by

$$S(q, \omega) \propto \left(a + \frac{4\pi N e^* b}{c^2 q^2 / \omega^2 - \epsilon_\infty} \right)^2 \frac{n(\omega) + 1}{(\epsilon_0 - \epsilon_\infty) \omega_0^2} \times \text{Im} \left(\frac{(c^2 q^2 / \omega^2 - \epsilon_\infty)^2}{c^2 q^2 / \omega^2 - \epsilon(\omega)} \right). \quad (1)$$

Here, a and b are the atomic displacement and electro-optical nonlinear susceptibility coefficients, respectively; N is the number of oscillators per unit volume; e^* is the transverse dynamic effective charge of the oscillator; ϵ_∞ is the optical dielectric constant; $n(\omega)$ is the Bose-Einstein thermal population factor; and $\epsilon(\omega)$ is the complex dielectric function. The first factor gives the relative scattering contributions from the phonon and photon parts of the polariton and modulates the integrated intensity, and the last factor is the dissipative part of the appropriate response function and determines the lineshape. For a damped single harmonic oscillator, the complex dielectric function can be written

$$\epsilon(\omega) = \epsilon_\infty + (\epsilon_0 - \epsilon_\infty) \omega_0^2 / [\omega_0^2 - \omega^2 - i\omega\gamma(\omega)], \quad (2)$$

where ϵ_0 is the low-frequency dielectric constant, ω_0 is the long-wavelength transverse optical phonon frequency, and $\gamma(\omega)$ is the damping constant which in general depends on frequency. Combining Eqs. (1) and (2), the total scattering cross section becomes

$$S(q, \omega) = S_0 [n(\omega) + 1] \left(1 + \frac{B}{c^2 q^2 / \omega^2 - \epsilon_\infty} \right)^2 \times \omega \gamma(\omega) \left\{ \left[\omega_0^2 \left(1 - \frac{\epsilon_0 - \epsilon_\infty}{c^2 q^2 / \omega^2 - \epsilon_\infty} \right) - \omega^2 \right]^2 + \omega^2 \gamma^2(\omega) \right\}^{-1}, \quad (3)$$

where S_0 is a nearly frequency-independent constant and $B = 4\pi N e^* b / a$ is the ratio of the electro-optical to the atomic displacement contribution to the Raman tensor. A result similar to this was obtained by Laughman, Davis, and Nakamura¹⁸ in the ferroelectric case where $\epsilon_0 \gg \epsilon_\infty$. The important features of Eq. (3) will become apparent if it is written in a slightly different form as

$$S(\omega_-, \omega) = S'_0 [n(\omega) + 1] \left(1 + \frac{B(\omega_0^2 - \omega_-^2)}{\omega_0^2(\epsilon_0 - \epsilon_\infty)} \right)^2 \times \frac{\omega_-^2 \omega \bar{\gamma} / \omega_0^2}{(\omega_-^2 - \omega^2)^2 + \omega^2 \bar{\gamma}^2}, \quad (4)$$

where

$$\omega_-^2 \equiv \omega_0^2 \left[1 + \left(\frac{\epsilon_0 - \epsilon_\infty}{c^2 q^2 / \omega^2 - \epsilon_\infty} \right)^{-1} \right] \quad (5)$$

and

$$\bar{\gamma} = (\omega_-^2 / \omega_0^2) \gamma(\omega_-). \quad (6)$$

Here, ω_- is the lower-polariton-mode frequency satisfying the dispersion relation in the absence of damping,

$$c^2 q^2 / \omega^2 = \epsilon^0(\omega) \equiv \epsilon_\infty + (\epsilon_0 - \epsilon_\infty) \omega_0^2 / (\omega_0^2 - \omega^2) \quad (7)$$

and $\bar{\gamma}$ is the *polariton* damping function, which is related to the *phonon* damping function $\gamma(\omega)$ by Eq. (4). This simple connection was also demonstrated by Loudon¹⁹ for the case of small damping $\gamma \ll \omega_0$ and large oscillator strength $\epsilon_0 \gg \epsilon_\infty$. Equation (7) is valid in the present case at low frequencies where the phonon contribution to ϵ_0 is dominated by the soft mode.

Next, it is necessary to relate the scattering angle to the polariton wave vector. Below $T = 492^\circ\text{C}$, PbTiO₃ is tetragonal with C_{4v} symmetry. The nonzero elements of the Raman tensor for the *E* modes are α_{xx} and α_{yz} .²⁰ The polarization (x, z) was used in order to observe the pure *E*-symmetry polariton. This leads to the incident light polarized ordinary ($\hat{e}_i = [100]$) and the scattered light polarized extraordinary ($\hat{e}_s = [001]$). From the conservation of energy and crystal momentum, one obtains

$$c^2 q^2 = \left[\omega_i (n_o - n_e) + \omega \left(n_e + \omega_i \frac{\partial n_e}{\partial \omega} \right) \right]^2 + \omega_i^2 n_e n_o \theta^2 \quad (8)$$

for the geometry used in the present experiment,

where ω_i is the incident laser frequency, n_o and n_e are the ordinary and extraordinary indices of refraction, respectively, and θ is the scattering angle as measured from the incident direction inside the crystal. The optical constants used in Eq. (8), $n_o = 2.670$ and $n_e = 2.662$, are given by Singh, Remika, and Polopowicz²¹ for similar crystals.

EXPERIMENTAL

The sample was a single crystal of PbTiO_3 approximately $5 \times 1 \times 1$ mm in size.²² In order to scatter from pure E -symmetry phonons below room temperature, the scattering geometry $y(xz)\bar{y}$ was used. The scattering geometry employed for observation of pure E -symmetry polaritons was $y(xz)y + \Delta z$, so the polariton was propagating in the $[001]$ pseudocubic direction and polarized in the $[100]$ direction.

The crystal was cut and polished on faces perpendicular to the $[010]$ axis to permit forward scattering. It was found to be single crystal in nature when observed through crossed polarizers and by strict compliance with Raman selection rules. The Raman-scattering experiment was performed on the sample using a 50-mW He-Ne laser operating at 6328 Å. The laser light was focused into the sample using a 100-cm focal length lens. A long focal length lens was used to minimize the divergence of the incident laser wave vector inside the scattering volume. For phonon-polariton scattering the light scattered in the near forward direction ($0.4^\circ < \theta < 5^\circ$) was collected by a 20-cm focal length lens. The collection optics had an adjustable stop aperture to limit the acceptance angle inside the crystal, $\Delta\theta$. The acceptance angles were varied from $\Delta\theta = 0.1^\circ$ to $\Delta\theta = 0.2^\circ$. The polarization of the collected light was selected by Polaroid film and then spectrally analyzed by a Spex Model 1400 double-grating spectrometer. The analyzed light was then detected by a cooled ITT model FW-130 photomultiplier with S-20 cathode. The spectrometer was controlled by a PDP-11 minicomputer which makes it possible to measure weak scattered signals by using very long integration times. The digitally stored data were then transferred to a large-memory computer where extensive analysis could take place.

The linewidth observed in a typical polariton scattering experiment arises from five principal contributions: (a) the intrinsic polariton damping, determined by the finite lifetime in a perfect crystal; (b) intrinsic broadening due to additional allowed scattering processes caused by crystal imperfections, impurities, domain walls, etc; (c) divergence of the incident and scattered beams

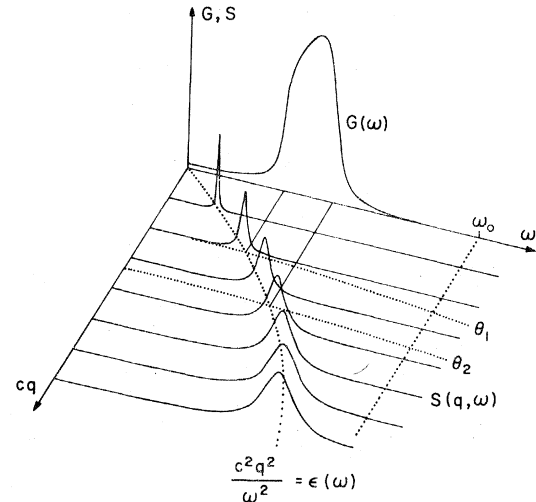


FIG. 1. Scattering intensity $S(q, \omega)$ as a function of wave vector cq and frequency ω for the soft E -symmetry polariton in PbTiO_3 . The dotted line from the origin is the polariton dispersion curve given by $c^2q^2/\omega^2 = \epsilon(\omega)$. The two dotted lines labeled θ_1 and θ_2 are the constant-angle curves described by Eq. (8) appropriate to a typical acceptance aperture of a polariton measuring apparatus. The solid line labeled $G(\omega)$ is the spectral shape of polaritons accepted between θ_1 and θ_2 and is derived from Eq. (9).

due to macroscopic crystal imperfections; (d) broadening due to the finite collection angle of the scattered light and hence finite range of wave vectors; and (e) broadening due to the finite resolution of the spectrometer. The quantity desired is (a), while (b) is usually small for bulk scattering. The effect of (c) was small since a collimated laser beam could easily pass through the thin (1-mm) sample without any visible distortion. The instrumental broadening due to (d) and (e) are in principle easy to remove from the experimental spectra. Illustrating the effect of (d) is Figure 1, a three-dimensional plot of $S(q, \omega)$. Only the light scattered between $\theta = \theta_1$ and $\theta = \theta_2$, relative to the forward direction, is allowed to pass through the acceptance slit into the spectrometer. The broadened spectrum $G(\omega)$ that enters the spectrometer is the sum of all the light scattered between the constant θ curves for θ_1 and θ_2 and is given by

$$G(\omega) = \int_{\theta_1}^{\theta_2} S(q(\theta), \omega) d\theta, \quad (9)$$

where $q(\theta)$ is given by Eq. (8). In the present case where the edges of the acceptance slit were not at constant scattering angles, a slightly more complicated integral was used with functional integration limits. The effect of (e) is to broaden the spectra further by the transfer function $T(\omega, \omega')$ of the spectrometer. The final measured spectrum

$I(\omega')$ is obtained by convoluting the initial spectrum with the transfer function as

$$I(\omega') = \int_0^\infty G(\omega) T(\omega, \omega') d\omega. \quad (10)$$

The transfer function is found by measuring the intensity spectrum when the input is a δ function in frequency, in this case the narrow ($\ll 1 \text{ cm}^{-1}$) laser line. For equal input and exit spectrometer slits, the slit profile is an isosceles triangle of full width at half-maximum (FWHM) W given by

$$T(\omega, \omega') = \begin{cases} (1/W)(1 - |\omega - \omega'|/W) & \text{for } |\omega - \omega'| < W \\ 0 & \text{otherwise.} \end{cases}$$

The independent parameters ϵ_0 , γ and a scaling factor

$$I_0 = S_0 \left(1 + \frac{B}{c^2 q^2 / \omega^2 - \epsilon_\infty} \right)^2$$

were successively adjusted to best fit while the intrinsic cross section of Eq. (3) was integrated twice to account for instrumental broadening. This method is similar to that employed by Ushioda and McMullen^{23,24} in which a simple Lorentzian lineshape was integrated analytically. However, in the present work, the integrations were performed numerically on a high-speed computer.

LOW-TEMPERATURE RESULTS

Results of the backscattering experiment below room temperature are shown in Fig. 2. This figure shows the temperature dependence of the soft

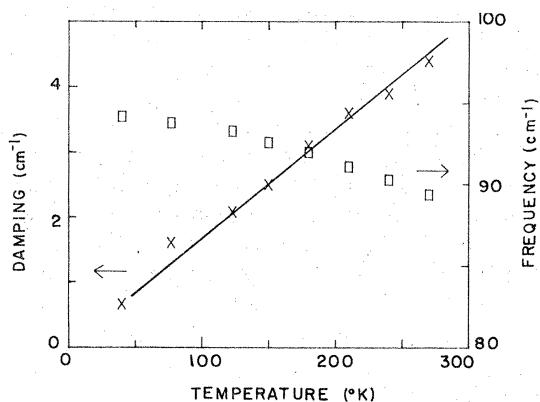


FIG. 2. Phonon frequency ω_0 vs absolute temperature T for the soft *E*-symmetry mode in PbTiO_3 is represented by squares. Phonon damping function $\gamma(\omega_0(T))$ vs absolute temperature T is represented by crosses. These results were obtained after removing the spectrometer resolution according to Eq. (10). The backscattering geometry $\gamma(\kappa z) \bar{y}$ was used. The solid curve is a straight line drawn through the origin and through the data points in order to aid the eye.

E-mode frequency $\omega_0(T)$ from 40 °K to room temperature. The variation in ω_0 is small and changes by only 5% over a 250 °K range. Figure 2 also shows the damping $\gamma(\omega_0, T)$ as a function of temperature. The damping decreases in a linear fashion with temperature and extrapolates to zero at absolute zero temperature. Thus, at nearly constant frequency the damping is proportional to the absolute temperature, at least from 40 °K to room temperature.

The values of γ represented here were obtained after removing the spectrometer resolution according to Eq. (10). Spectrometer slit settings were chosen to give values for W of 0.75 cm^{-1} and 1.5 cm^{-1} . The reliability of the deconvoluting procedure was tested by comparing the results of γ from different slit settings. At lower temperatures, where the value of γ was comparable to W , both of the slit settings were used and gave nearly identical values for γ . During the entire course of the run, care was taken to insure that the same region of the sample was examined, since the damping was found to fluctuate by about 20% over the volume of the sample. This variation is probably attributable to the intrinsic broadening effects of (b). The data displayed in Fig. 2 are chosen from the run that had the lowest γ at lower temperatures.

POLARITON RESULTS AT ROOM TEMPERATURE

At constant temperature, the frequency dependence of γ is found through measurement of the polariton damping at different scattering angles in the near-forward direction.²⁵ The phonon damping $\gamma(\omega, T_{\text{rm}})$ is determined and is then associated with the corresponding polariton frequency ($\omega = \omega_-$).

Figure 3 shows a spectrometer trace for a polariton at $cq = 650 \text{ cm}^{-1}$ and $\omega_- = 56 \text{ cm}^{-1}$. An estimate of the phonon damping can be found by removing the instrumental resolution from the FWHM. Deconvoluting the spectrometer resolution ($W = 2.8 \text{ cm}^{-1}$) from the FWHM of the polariton line shape, $\Delta\omega = 7.6 \text{ cm}^{-1}$, results in a linewidth of $\Delta\omega = 6.5 \text{ cm}^{-1}$. The acceptance angle of scattered light $\Delta\theta = 0.002$, reduces the FWHM to 3.4 cm^{-1} . Finally, the phonon damping derived from Eq. (6) is $\gamma = 8.6 \text{ cm}^{-1}$. This value of the phonon damping is associated with a frequency of 56 cm^{-1} .

The results of the soft-phonon damping function as a function of frequency at room temperature are plotted in Fig. 4. $\gamma(\omega)$ increases with decreasing ω . Also plotted in Fig. 4 are the results of Burns and Scott,⁷ $\gamma(\omega_0(T))$, which contains both temperature dependence and frequency dependence through the variation of the soft-mode frequency $\omega_0(T)$ with temperature. The decrease in $\omega_0(T)$

corresponds to higher temperatures close to T_c .

The values for $\gamma(\omega, T_{\text{rm}})$ were determined for various scattering angles using frequency-independent damping. These values were then fitted to the function

$$\gamma(\omega) = A\Gamma / [(40 - \omega)^2 + \Gamma^2] + 4, \quad (11)$$

where A is the magnitude of a resonant contribution centered at 40 cm^{-1} with width Γ . This function is shown in Fig. 4, where $A = 150$ and $\Gamma = 15 \text{ cm}^{-1}$. Since each polariton peak extends over a small frequency range, almost identical results were found for $\gamma(\omega)$ when the experimental lineshapes were fitted with either constant damping or frequency dependent damping.

For cubic anharmonicity, the imaginary part of the self energy is¹ proportional to

$$n(\omega_1) + n(\omega_2) + 1 \quad \text{for } \omega_0 = \omega_1 + \omega_2$$

or

$$n(\omega_1) - n(\omega_2) \quad \text{for } \omega_0 = \omega_2 - \omega_1,$$

corresponding to decay and scattering of the soft mode, respectively, and is responsible for the major part of the temperature dependence. Since $kT_{\text{rm}} \cong 208 \text{ cm}^{-1}$, the high-temperature approximation for the Bose-Einstein factor is valid and $n(\omega) \approx kT/\hbar\omega$. Then it is expected that $\gamma(\omega, T)$ is proportional to T at fixed ω , if the dominant damping mechanism of the soft mode is due to third-order anharmonicity in the crystal potential energy. (Higher-order effects will produce a T^2 or higher power dependence.) The results of the damping at low temperatures indicate that the dominant

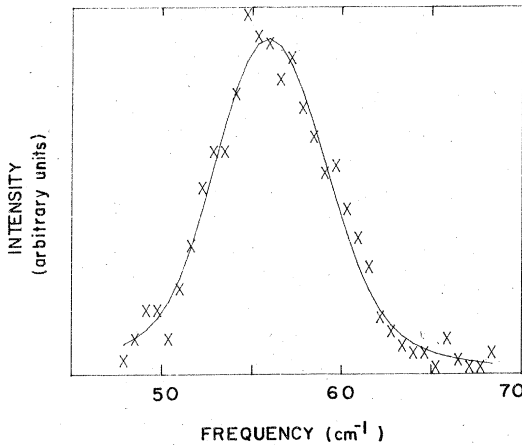


FIG. 3. Scattering intensity vs frequency for the soft E -symmetry polariton in PbTiO_3 at $cq = 650 \text{ cm}^{-1}$. The crosses represent the unsmoothed experimental data and the solid curve is the best fit to Eq. (3) with convolutions of Eqs. (9) and (10).

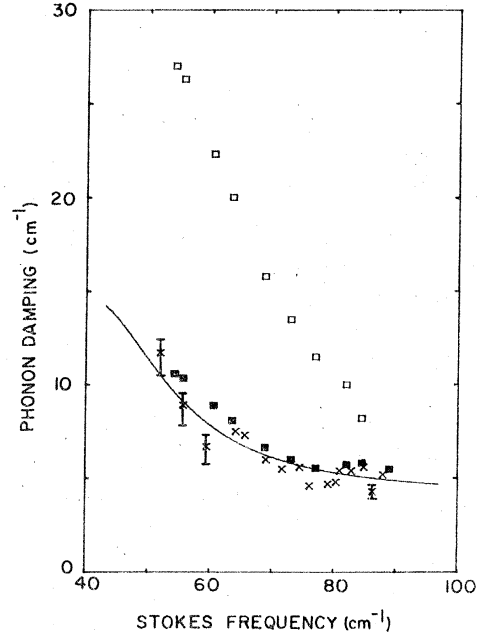


FIG. 4. Frequency vs phonon damping for the soft E -symmetry mode in PbTiO_3 . The crosses represent the polariton data measured at room temperature in the present experiment. The solid curve is Eq. (11) fitted to the data. The open squares represent $\gamma(\omega_0(T))$ taken between room temperature and $T_c = 493^\circ\text{C}$. The solid squares are the temperature-dependent data reduced by Eq. (12). Typical error bars are indicated and are derived from the uncertainty in the curve fitting.

mechanism responsible is indeed due to a three-phonon decay or scattering process. If the damping at constant frequency is linear with temperatures and if no temperature-dependent anomaly exists, then the relation

$$\gamma(\omega, T_{\text{rm}}) = (T_{\text{rm}}/T)\gamma(\omega_0(T)) \quad (12)$$

should hold for $\omega = \omega_0(T)$, and the left-hand side is the value measured in the present work at T_{rm} . $\gamma(\omega_0(T))$ on the right-hand side is the value measured by Burns and Scott at T . Figure 4 shows the comparison of the left- and right-hand side of Eq. (12). It is seen that Eq. (12) holds without any adjustable parameters for all ω and T measured. Note that because of the large uncertainty in linewidth measurements, a smaller nonlinear dependence (T^2) may exist.

The polariton fitting procedure also gave a value for $\epsilon_a(0)$ and the integrated intensity. The value of the low-frequency dielectric constant along a direction perpendicular to the ferroelectric c axis was found to depend slightly on the polariton frequency. This dependence is attributed to the error introduced by selecting a single oscillator model for the dielectric function instead of the more com-

plicated triple oscillator model. Because of the large strength of the lowest mode and the low frequency region under consideration, the dielectric properties given by a single oscillator model closely approximates the more general three-oscillator model. A value of $\epsilon_a(0) = 85 \pm 5$ was found by extrapolating the polariton dispersion curve to zero frequency. This value varied from sample to sample and was the highest obtained. This is somewhat lower than the value of 107 derived from the LST relation.⁷ The integrated intensity varied by less than 30% between $\omega_- = 55 \text{ cm}^{-1}$ and $\omega_0 = 89 \text{ cm}^{-1}$. Since the integrated intensity should be proportional to

$$\left(1 + \frac{B}{c^2 q^2 / \omega^2 - \epsilon_\infty}\right)^2,$$

this implies that $1 + B\omega_-^2/c^2 q^2 \approx \text{constant}$ or that $|B| < c^2 q^2 / \omega_-^2$. Thus,

$$|B| = |4\pi N e^* b / a| < \epsilon_a(0),$$

or the ratio of the atomic displacement contribution to the Raman tensor, relative to the electro-optical contribution, is less than 10^2 .

DISCUSSION OF RESULTS

The results obtained here support the following description for divergent damping of soft modes. The most important thing is that the transition occurs as a consequence of the anharmonicity. As the temperature is raised, all anharmonic processes become stronger, allowing not only the phonon damping to increase but also a shift to lower phonon frequency. Since anharmonic decay processes rely on conserving energy between the phonons involved, a stronger energy overlap or more nearly resonant condition exists as the phonon frequency approaches such a resonance. The linearlike temperature dependence of the damping implies that the soft mode decays by interaction with two large wave vector phonons.

Several important conclusions can be drawn concerning the nature of the soft-mode damping function and consequently the imaginary part of the self-energy. At constant frequency, the damping is proportional to the absolute temperature, from 40 to 300 °K, and approximately linear from 300 to 766 °K, although more uncertain. This asymptotic linear T dependence is also seen in²⁶ GaP and²⁷ CuI below room temperature.

The results of a microscopic theory of anharmonicity⁴ show that this simple temperature dependence implies that the major contribution to the damping arises from cubic anharmonicity in the lattice potential energy. In other words, the finite lifetime of the soft mode is due to a scat-

tering or decay mechanism involving two other phonons. Also, the apparent divergence of γ for T approaching T_c from below in PbTiO₃ is caused by two important factors: (i) at fixed frequency, γ increases linearly with the absolute temperature, and (ii) ω_0 decreases as T is increased toward T_c and moves into a frequency region where $\Gamma(\omega)$ is large. (It must be noted that because of the uncertainty associated with measurements of damping, nonlinear T dependence cannot be ruled out completely.)

The next question to be considered is why $\gamma(\omega)$ increases as the frequency decreases. The first and most probable cause is a nearly resonant condition of ω_0 with a linear combination of other phonons. Cowley¹ has calculated the frequency dependence of $\Gamma(\omega, T)$ at several temperatures for simple crystals, revealing that for cubic anharmonic effects $\Gamma(\omega)$ has a form similar to the two-phonon density of states $\rho_2(\omega)$ at the Brillouin-zone center ($q=0$). That is, there are peaks in Γ associated with combinations of high one-phonon density of states which are mostly at zone boundaries. By inspecting the inelastic neutron scattering data,²⁸ one sees that a peak in $\rho_2(\omega)$ may be expected at $33 \pm 5 \text{ cm}^{-1}$. This peak derives from two zone-boundary phonons, TA and LA, with frequencies of 75 and 108 cm^{-1} , respectively. The damping process that corresponds to this peak in Γ is the scattering of the soft phonon by a TA (X) phonon (75 cm^{-1}) into an LA (X) (108 cm^{-1}). Infrared absorption indicates that there is a peak in the absorption spectrum at about 40 cm^{-1} at room temperature which may arise from a peak in $\rho_2(\omega)$.²⁹

Tani³⁰ has proposed another explanation for increased damping as ω_0 softens. He attributes this to "critical slowing-down" of fluctuations in the order parameter. Increased damping is attributed to an increase in the amplitude of vibration as the soft mode frequency decreases. As the transition is approached, the vibrational amplitude of the ions associated with the soft mode increases, and the ions travel farther from their equilibrium positions where the anharmonicity in the crystal potential energy is larger. This can result in domination by higher-order anharmonic terms in the crystal potential, allowing four phonon and higher decay interactions. In transitions that are strongly first order, the effect of critical slowing-down may be small since ω_0 is not allowed to soften to near zero as in a second order transition. Another result of these effects is that the damping would not only diverge below T_c but might also diverge above T_c while "decreasing" the temperature toward T_c . Fleury and Worlock⁵ have measured γ as a function of T for the ferroelectric modes in KaTaO₃ and SrTiO₃ above their incipient

transitions ($T_c < 0$ K). These materials did not show any increased damping or other anomalous behavior near T_c . KaNbO_3 shows a linear T dependence in $\gamma(T)$, while SrTiO_3 shows an unusual $T^{3/2}$ dependence.

A third explanation for divergent damping is given by Lockwood and Torrie.⁹ It appears that the large increase in the soft-mode linewidth in KMnF_3 as $T \rightarrow T_c^-$ results not directly from $\gamma(T)$ but arises from additional quasielastic scattering at very low frequencies. They found that the soft-mode damping parameter is essentially proportional to T but very near the transition ($T_c - T < 10$ K) additional scattering is allowed by "phonon density fluctuations." The result is that not only the normal collective-type mode is present but additional scattering occurs centered about zero frequency with a Debye relaxation-type spectrum. If the soft phonon mode is overdamped, these two structures will in general not be resolvable and would appear as one mode with anomalous $\gamma(T)$ and $\omega_0(T)$. This may not apply since the soft E mode in PbTiO_3 is underdamped at all temperatures.

High-pressure Raman scattering studies on PbTiO_3 at room temperature by Cerdeira *et al.*³¹ show that the damping does not diverge for ω_0 as low as 45 cm^{-1} . These results do not contradict the proposed phonon decay picture. High pressure not only alters the zone center phonon frequencies, but also the zone boundary frequencies, thereby shifting the frequency of most decay channels. The difference between the zone boundary phonon frequencies providing the decay channel might also change. When off resonance, the residual damping will be provided by a third-order nonresonant background. The application of hydrostatic pressure may in some cases cause a phonon to become resonant with a decay channel not ordinarily allowed at atmospheric pressure. Such a resonant condition would bring about a phase transition in much the same manner as changing the temperature. Many materials undergo such phase transitions at high pressure.

There is an apparent contradiction between structure in $\gamma(\omega)$ at room temperature and line-shape fits at higher temperatures.³² At temperatures close to T_c , the phonon line shapes are well fit by assuming a constant frequency-independent damping. These results⁷ were also confirmed by high-temperature studies on our own samples. Thus we can rule out any sample dependence. Our room-temperature results for $\gamma(\omega)$ are consistent with room-temperature phonon line shapes because the damping is nearly constant over the frequency range of the phonon profile, $\Delta\omega \sim 20 \text{ cm}^{-1}$. Because of the uncertainties involved ($\pm 30\%$), the relation $\gamma(\omega, T) = T\gamma(\omega)$ is expected to hold only approxima-

tely, especially near T_c . In general, we do not expect $\gamma(\omega)$ to have the same frequency dependence at all temperatures; at higher temperatures this structure in γ may spread out. If this structure arises from the lifetime along with the dispersion of the phonons contributing to the decay channel, any peak in $\gamma(\omega)$ will broaden with temperature.

DIVERGENT DAMPING IN RELATED TRANSITIONS

The damping of the lowest A_1 mode in $\text{Gd}_2(\text{MoO}_4)_3$, was seen to diverge as $T \rightarrow T_c$, while ω_0 decreased only slightly.¹¹ Recently, the same divergent behavior was also seen by applying uniaxial stress. The damping decreased strongly with increasing stress while ω_0 increased slightly.³³ In both cases, the damping increased rapidly while ω_0 decreased only a small amount. Thus, it seems that the application of stress affects the lattice vibrations in much the same manner as changing the temperature. These properties fit the model of phonon resonance decay reasonably well. In this case, the soft-mode frequency moves away from a decay resonance as the pressure increases. Another description is that T_c effectively increases with pressure, implying that more anharmonicity due to thermal vibrations is needed to drive the soft-mode frequency down to the decay resonance. This agrees with the results that T_c increases strongly with increasing hydrostatic pressure.³⁴ Therefore, the divergent behavior of γ may be explained by (i) intrinsic frequency-dependent damping, where ω_0 is changed either by changing the temperature or by applying stress, or (ii) an effect proportional to $T_c - T$ rather than dependent on the absolute temperature alone.

The apparent divergence in $\gamma(T)$ evident in $^6\text{GeTe}$ and³⁵ $\text{Gd}_2(\text{MoO}_4)_3$ may be complicated by the presence of other features close to the soft mode. The soft E mode in GeTe appears to be a single underdamped mode which shows normal linear dependence of $\gamma(T)$. The A_1 -mode spectrum of GeTe shows a small peak at slightly lower frequency in addition to the soft mode. The linewidth shows normal linear T dependence below room temperature where the low-frequency modes are clearly resolvable. Above room temperature, the two modes overlap and the linewidth of this feature then diverges. So it is not completely clear whether $\gamma(T)$ of the soft A_1 -mode in GeTe actually diverges or shows normal linear behavior. In any case, linear temperature dependence is clearly observable over certain regions. These extra features that lie just below the soft mode may not be vibrational modes at all, but features caused by interactions of the soft mode with decay resonances.³⁶

In the case of the closely related perovskite BaTiO_3 , the damping Γ of the soft E mode decreases with frequency below $\omega_0 = 33 \text{ cm}^{-1}$.³⁷ Inelastic neutron scattering data³⁸ show that it is underdamped for $\omega_0(q) > 33 \text{ cm}^{-1}$, corresponding to finite q values. Thus, it appears that both in BaTiO_3 and in PbTiO_3 there is a peak in the $\Gamma(\omega)$ near 30 cm^{-1} . The soft-mode frequency in PbTiO_3 lies far from a peak in Γ while the corresponding lowest E -mode frequency in BaTiO_3 happens to lie near a corresponding peak in $\Gamma(\omega)$. This may be the reason why the soft mode is overdamped in BaTiO_3 and underdamped in PbTiO_3 . Lefkowitz³⁹ has attributed the large damping of the lowest E mode in BaTiO_3 to a scattering mechanism involving two acoustic modes seen with inelastic neutron scattering.

More information on the dissipative contribution to the phonon self-energy $\Gamma(\omega, T)$ will eventually lead to a better understanding of the dispersive

contribution $\Delta(\omega, T)$ and hence on the softening of vibrational modes associated with phase transitions. (The real and imaginary parts of the self-energy are related by a Kramers-Kronig transform.) In materials exhibiting strongly first-order phase transitions, $\omega_0(T)$ is accurately known below T_c but usually does not show a Curie-like behavior. A knowledge of $\Delta(\omega, T)$ and the order parameter may not only explain this deviation but also single out the mechanisms inducing the change to a new phase.

ACKNOWLEDGMENTS

The authors are grateful to Dr. J. P. Remeika of Bell Laboratories for providing the excellent crystals of PbTiO_3 . Many stimulating discussions with Professor A. A. Maradudin and Professor D. L. Mills are appreciated. This work was supported in part by NSF Grant Nos. DMR 73-02480 and DMR 77-10083.

*Present address: Dept. of Physics, University of Southern California, University Park, Los Angeles, Calif. 90007.

¹R. A. Cowley, *Adv. Phys.* **12**, 421 (1963).

²R. A. Cowley, *Philos. Mag.* **11**, 673 (1965).

³A. D. Bruce and R. A. Cowley, *J. Phys. C* **6**, 2422 (1973).

⁴A. A. Maradudin and A. E. Fein, *Phys. Rev.* **128**, 2589 (1962).

⁵P. A. Fleury and J. M. Worlock, *Phys. Rev.* **174**, 613 (1968).

⁶E. F. Steigmeier and G. Harbeke, *Solid State Commun.* **8**, 1275 (1970).

⁷G. Burns and B. A. Scott, *Phys. Rev. B* **7**, 3088 (1973).

⁸E. F. Steigmeier and H. Auderget, *Solid State Commun.* **12**, 565 (1973).

⁹D. J. Lockwood and B. H. Torrie, *J. Phys. C* **7**, 2729 (1974).

¹⁰W. Dultz, M. Quilichini, J. F. Scott, and G. Lehmann, *Phys. Rev. B* **11**, 1648 (1975).

¹¹P. A. Fleury, *Solid State Commun.* **8**, 601 (1970).

¹²J. F. Ryan and J. F. Scott, *Solid State Commun.* **14**, 5 (1974).

¹³G. Burns and B. A. Scott, *Phys. Rev. Lett.* **25**, 167 (1970).

¹⁴B. D. Silverman, *Solid State Commun.* **10**, 311 (1972).

¹⁵M. DiDomenico, S. H. Wemple, S. P. S. Porto, and R. P. Bauman, *Phys. Rev.* **174**, 522 (1968).

¹⁶H. J. Benson and D. L. Mills, *Phys. Rev. B* **1**, 4835 (1970).

¹⁷A. S. Barker, Jr. and R. Loudon, *Rev. Mod. Phys.* **44**, 18 (1972).

¹⁸L. Laughman, L. W. Davis, and T. Nakamura, *Phys. Rev. B* **6**, 3322 (1972).

¹⁹R. Loudon, *J. Phys. A* **3**, 233 (1970).

²⁰R. Loudon, *Adv. Phys.* **13**, 423 (1964).

²¹S. Singh, J. P. Remeika, and J. R. Polopowicz, *Appl.*

Phys. Lett. **20**, 135 (1972).

²²J. P. Remeika and A. M. Glass, *Mater. Res. Bull.* **5**, 37 (1970).

²³S. Ushioda and J. D. McMullen, *Solid State Commun.* **11**, 299 (1972).

²⁴S. Ushioda and J. D. McMullen, in *Polaritons, Proceedings of the First Taormina Research Conference on the Structure of Matter*, edited by E. Burstein and F. DeMartini (Pergamon, New York, 1974), p. 77.

²⁵D. Heiman, S. Ushioda, and J. P. Remeika, *Phys. Rev. Lett.* **34**, 886 (1975).

²⁶S. Ushioda, J. D. McMullen, and M. J. Delaney, *Phys. Rev. B* **8**, 4634 (1973).

²⁷T. Fukumoto, K. Tabuchi, S. Nakashima, and A. Mituishi, *Opt. Commun.* **10**, 78 (1974).

²⁸G. Shirane, J. D. Axe, J. Harada, and J. D. Remeika, *Phys. Rev. B* **2**, 155 (1970).

²⁹J. Stevens and R. Braunstein (private communication).

³⁰K. Tani, *J. Phys. Soc. Jpn.* **26**, 93 (1969).

³¹F. Cerdeira, W. B. Holzapfel, and D. Bauerle, *Phys. Rev. B* **11**, 1188 (1975).

³²G. Burns, *Phys. Rev. Lett.* **37**, 229 (1976).

³³F. G. Ullman, B. N. Ganuly, J. R. Hardy, and R. D. Kirby, in *Proceedings of the Third International Conference on Light Scattering in Solids*, Campinas, Brazil, 1975 (unpublished).

³⁴A. M. Shirokov, *Fiz. Tverd. Tela* **13**, 3108 (1971) [*Sov. Phys.-Solid State* **13**, 2610 (1971)].

³⁵T. Shigenari, Y. Takagi, and Y. Wakabayashi, *Solid State Commun.* **18**, 1271 (1976).

³⁶J. Ruvalds and A. Zawadowski, *Phys. Rev. B* **2**, 1172 (1970).

³⁷D. Heiman and S. Ushioda, *Phys. Rev. B* **9**, 2122 (1974).

³⁸G. Shirane, J. D. Axe, and J. Harada, *Phys. Rev. B* **2**, 3651 (1970).

³⁹I. Lefkowitz, *Proc. Phys. Soc. Lond.* **80**, 868 (1962).